

DYNAMIC MECHANICAL PROPERTIES OF NATIVE ENDPLATE

Josef Šepitka

Czech Technical University in Prague, Faculty of Mechanical Engineering, Prague, Czech Republic

Abstract

A study of mechanical properties of native tissues is a great challenge in biomechanics. Especially, hardly accessible structures that play a very important role within a locomotive system. A study of a cartilaginous endplate (CEP) is just such a challenge. CEP is approximately 0.6 mm thin layer of hyaline cartilage between an intervertebral disc (IVD) and a vertebral body (VB). A calcification or any mechanical damage of CEP can cause restrictions of nutrition and metabolic waste flow inward and outward from IVD, respectively. Degenerative processes influence mechanical properties of the tissue. Due to very small thickness of CEP, instrumental nanoindentation seems to be suitable method for this task. This paper presents a study of time dependent viscoelastic properties of native porcine CEP using nanoscale dynamic mechanical analysis in the range of frequency from 5 Hz to 215 Hz. The storage moduli were obtained in the range from 11.78 MPa to 17.11 MPa. The loss moduli were obtained in the range from 2.96 MPa to 5.32 MPa.

Keywords

viscoelastic properties, mechanical properties, dynamic mechanical analysis, cartilaginous endplate

Introduction

Back pain is one of the main problems of Western industrialized countries. The number of people affected by these problems is between 12% and 35%. This disability causes an economic burden on society. The total losses caused by health care costs due to lost productivity and reimbursement of sickness benefits are estimated at 1.1% of gross domestic product in Great Britain and even 1.7% of gross domestic product in the Netherlands [1].

Cartilaginous end plate (CEP) is a part of intervertebral disc that creates the transition zone between hard vertebral body (VB) and soft anulus fibrosus (AF). The process of calcification within AF lamellae and CEP is crucial for mechanical behavior of intervertebral disc (IVD) [2]. Calcification of IVD was observed as the clinical syndrome in childhood and elderly population [3]. Sometimes the etiology is unclear. The previous trauma, surgical intervention or overloading are suggested. Calcification of CEP has critical influence on solutes flow to avascular AF and nucleus pulposus (NP) and initiates the IVD degeneration [4].

Machining of biological material to normalized shaped samples for tensile testing is quite difficult. According to recent studies the nanoindentation seems to be a very effective tool to analyze mechanical properties of biomaterials especially in case of hardly accessible soft tissue [5].

The storage modulus (E') as elastic response, loss modulus (E'') as viscoelastic response, and $\tan \delta$ as damping of the sample in the non-destructive time dependent deformation range can be determined by nanoscale dynamic mechanical analysis (nanoDMA) [5, 6].

This paper presents a study of time dependent viscoelastic properties of native porcine intervertebral disc's endplate using nanoscale dynamic mechanical analysis.

Methods

Sample preparation

A porcine cartilaginous endplate of lumbar spine L4 was used in our study. The spine was obtained from a butchery at the day of testing. The lumbar spine motion segments were immediately dissected and ten-millimeter-thick plates of vertebral body, end plate and annulus fibrosus were cut and polished under running water condition. Specimen was glued to the bottom of the Petri dish and surrounded by phosphate-buffered saline (PBS). The surface of the sample was under PBS and ready to be indented under a water level.

Testing condition

NanoDMA load controlled experiment was performed on Hysitron TriboIndenter™ system (Bruker Corp.,

USA) with diamond conospherical fluid cell probe with tip radius 10 μm at the temperature 22.9 °C.

Harmonic loading with dynamic load amplitude 1 μN superimposed to constant force $P_{max} = 200 \mu\text{N}$ was specified for harmonic frequency in the range from 5 to 215 Hz.

Values of damping C_i and stiffness K_i of machine were determined during air indent calibration. The procedure was adopted from Asif et. al. (1999) as well as the analysis of dynamic data [6].

Theory of nanoDMA

Dynamic driving force $P_0 \sin(\omega t)$ with amplitude P_0 and frequency $f = \omega/2\pi$ is superimposed on quasistatic loading P_{max} and stands for particular term in an equation of motion of the indenter relative to the indenter head:

$$P_0 \sin(\omega t) = m\ddot{x} + C\dot{x} + Kx. \quad (1)$$

The solution to the above equation, where compliance $C = C_i + C_s$ and stiffness $K = K_i + K_s$ of the system in Fig. 1 are defined respectively, is a steady-state displacement oscillation at the same frequency as the harmonic loading

$$x = X_0 \sin(\omega t - \Phi), \quad (2)$$

where X_0 is the amplitude of the displacement oscillation and Φ is the phase shift of the displacement with respect to the driving force. Both terms in Eq. 2 are recorded by the nanoindentation system.

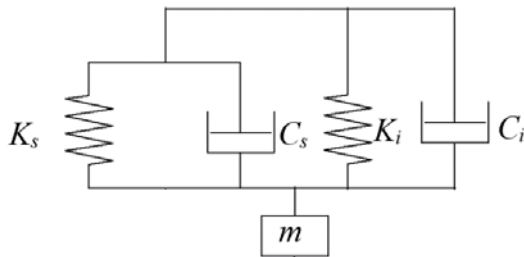


Fig. 1: Rheological model of indenter system where K_s is the contact stiffness, C_s is the damping coefficient of the specimen, K_i is the spring constant of the leaf springs that hold the indenter shaft, C_i is the damping coefficient of the air gap in the capacitive displacement sensor, m is the indenter mass.

The standard analytical solution for the model in Fig. 1, that assumes that the machine frame stiffness K_i is infinite, follows.

The amplitude of the displacement signal X_0 and the phase shift between force and displacement Φ are given by

$$X_0 = \frac{P_0}{\sqrt{(K_s + K_i - m\omega^2)^2 + [(C_i + C_s)\omega]^2}}, \quad (3)$$

$$\Phi = \tan^{-1} \frac{(C_i + C_s)\omega}{K_s + K_i - m\omega^2}, \quad (4)$$

where m is the indenter mass, ω is the frequency in rad/s, C_i is the damping coefficient of the air gap in the capacitive displacement sensor, C_s is the damping coefficient of the specimen, K_i is the spring constant of the leaf springs that hold the indenter shaft and K_s is the contact stiffness [6].

These calculated values for stiffness and damping of the sample are then used for determination of the viscoelastic properties of reduced storage modulus (E_r'), loss modulus (E_r'') and $\tan \delta = E_r'/E_r''$.

$$E_r' = \frac{K_s \sqrt{\pi}}{2\sqrt{A_c}}, \quad (5)$$

$$E_r'' = \frac{\omega C_s \sqrt{\pi}}{2\sqrt{A_c}}, \quad (6)$$

$$\tan \delta = \frac{C_s \omega}{K_s}, \quad (7)$$

where A_c is the contact area based on tip area function related to the contact depth at quasistatic loading [6]. The storage and loss modulus of the sample E_s' and E_s'' , respectively, are related to the reduced storage and loss modulus by

$$\frac{1}{E_r'} = \frac{(1-\nu_i^2)}{E_i} + \frac{(1-\nu_s^2)}{E_s'}, \quad (8)$$

$$\frac{1}{E_r''} = \frac{(1-\nu_i^2)}{E_i} + \frac{(1-\nu_s^2)}{E_s''}, \quad (9)$$

where subscripts i and s refer to the indenter and sample materials, respectively, and ν is the Poisson's ratio [7].

The storage modulus and the loss modulus are related to the complex modulus $E_s^* = E_s' + iE_s''$ and indicate the ability of the sample to store and return energy (recoverable deformation; E_s') and dissipate energy (E_s''). The ratio of the loss modulus to the storage modulus (i.e., $\tan \delta$) reflects the viscoelastic behavior of the material. It is a material parameter independent of the tip-sample contact area.

Results

The storage modulus increases from $E' = 11.78 \pm 4.87 \text{ MPa}$ to $E' = 17.11 \pm 6.41 \text{ MPa}$ up to the frequency 110 Hz (Fig. 2). Storage modulus then slowly decreases to the value $E' = 13.59 \pm 4.60 \text{ MPa}$ with increasing frequency. The loss modulus has similar trend in the beginning of the frequency characteristic. E'' increases up to the frequency 131 Hz from $E'' = 2.96 \pm 1.09 \text{ MPa}$ up to $E'' = 4.88 \pm 1.38 \text{ MPa}$

(Fig. 3). Loss modulus drops to $E'' = 4.07 \pm 1.29$ MPa at the frequency 152 Hz afterwards. Loss modulus then increases up to maximum value $E'' = 5.32 \pm 1.38$ MPa at the frequency 215 Hz. $\tan \delta$ has increasing trend in whole frequency range except the frequency 152 Hz where value drops from 0.36 ± 0.05 to 0.28 ± 0.05 (Fig. 4).

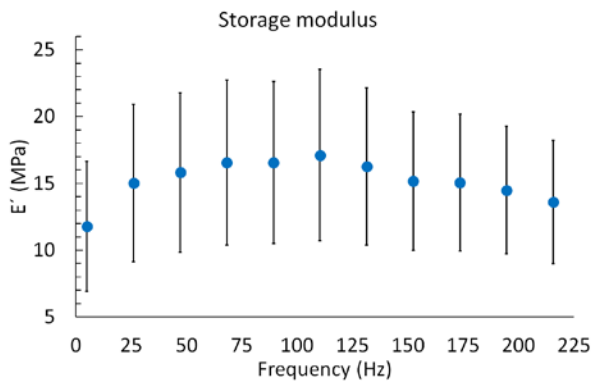


Fig. 2: Frequency sweep of storage modulus.

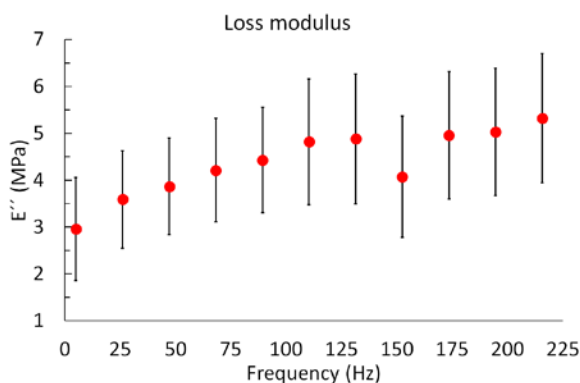


Fig. 3: Frequency sweep of loss modulus.

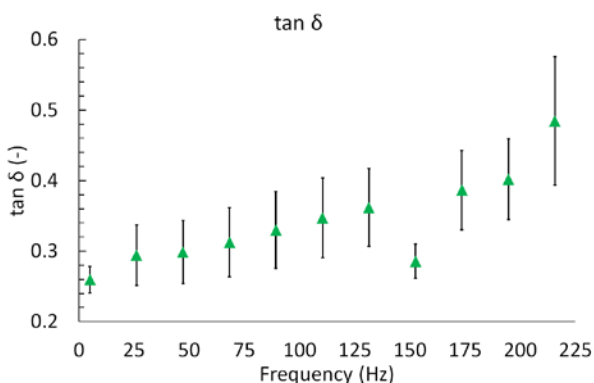


Fig. 4: Frequency sweep of damping.

Discussion

The endplate is able to store maximum portion of energy at the frequency 110 Hz (Fig. 2). At higher frequencies, the modulus value slightly decreases. Loss modulus increases up to the frequency 110 Hz, then the trend is almost constant up to frequency 131 Hz where value drops to the local minimum at the frequency 152 Hz, which is followed by an increase of values with increasing frequency up to the maximum of E'' .

The loss modulus has increasing trend in whole range of the frequencies except the frequencies between 131–152 Hz where values dramatically decreased. This phenomenon is probably related to the inflex point at the maximum of storage moduli and shows the consequence of deformation energy dissipation inside the endplate. The increase of $\tan \delta$ with increasing loading rates can be associated with the localized softening of the endplate [8]; except the frequency between 131–152 Hz where is evident local drop of the values.

Measured values and trend of $\tan \delta$ are in agreement with Sepitka et al. [8]. There are not any available data to compare values of storage and loss moduli of native fully lubricated endplate in the present. Franke et al. [5] obtained frequency sweep data of native porcine articular cartilage using nanoDMA in the range of frequencies from 1 to 250 Hz. Their storage moduli E' and loss moduli E'' were in the range from 3 MPa to 16 MPa and in the range from 3 MPa to 4.5 MPa, respectively, which is in agreement with our measured values. However, Franke et al. have increasing trend of mechanical properties with increasing frequency compared to our results [5]. These differences in the frequency sweep trends could be caused by the influence of different internal microstructure of the compared samples [8]. It would be appropriate to analyze the influence of the internal microstructure on the local mechanical properties of the native endplate.

Conclusion

Nanomechanical testing of native cartilaginous endplate by nanoscale dynamic mechanical analysis was done successfully. We obtained frequency sweeps of mechanical properties in the range of frequencies from 5 Hz to 215 Hz. Cartilaginous endplate has time dependent mechanical properties. Storage modulus increases up to the frequency 110 Hz then starts to decrease slightly. Loss modulus increases up to the frequency 110 Hz, then the trend is almost constant up to frequency 131 Hz where value drops to the local

minimum at the frequency 152 Hz which is followed by an increase of values with increasing frequency up to the maximum value of E'' . The storage moduli were obtained in the range from 11.78 ± 4.87 MPa to 17.11 ± 6.41 MPa. The loss moduli were obtained in the range from 2.96 ± 1.10 MPa to 5.32 ± 1.38 MPa.

Acknowledgement

The work has been supported by Grant Agency of the Czech Technical University in Prague, grant No. SGS22/149/OHK2/3T/12.

References

- [1] Urban JP, Roberts S. Degeneration of the intervertebral disc. *Arthritis Res Ther.* 2003;5(3):120–30. DOI: [10.1186/ar629](https://doi.org/10.1186/ar629)
- [2] Melrose J, Burkhardt D, Taylor TK, Dillon CT, Read R, Cake M, et al. Calcification in the ovine intervertebral disc: a model of hydroxyapatite deposition disease. *Eur Spine J.* 2009 Apr;18(4):479–89. DOI: [10.1007/s00586-008-0871-y](https://doi.org/10.1007/s00586-008-0871-y)
- [3] Chanchairujira K, Chung CB, Kim JY, Papakonstantinou O, Lee MH, Clopton P, et al. Intervertebral disk calcification of the spine in an elderly population: radiographic prevalence, location, and distribution and correlation with spinal degeneration. *Radiology.* 2004 Feb;230(2):499–503. DOI: [10.1148/radiol.2302011842](https://doi.org/10.1148/radiol.2302011842)
- [4] Peng B, Hou S, Shi Q, Jia L. The relationship between cartilage end-plate calcification and disc degeneration: an experimental study. *Chin Med J (Engl).* 2001 Mar;114(3):308–12.
- [5] Franke O, Goken M, Meyers MA, Durst K, Hodge AM. Dynamic nanoindentation of articular porcine cartilage. *Mater Sci Eng C.* 2011 May 10;31(4):789–95. DOI: [10.1016/j.msec.2010.12.005](https://doi.org/10.1016/j.msec.2010.12.005)
- [6] Seyed Asif SA, Wahl KJ, Colton RJ. Nanoindentation and contact stiffness measurement using force modulation with a capacitive load-displacement transducer. *Rev Sci Instrum.* 1999 May 1;70(5):2408–13. DOI: [10.1063/1.1149769](https://doi.org/10.1063/1.1149769)
- [7] Oliver WC, Pharr GM. An improved technique for determining hardness and elastic modulus using load and displacement sensing indentation experiments. *J Mater Res.* 1992 Jun;7(6):1564–83. DOI: [10.1557/JMR.1992.1564](https://doi.org/10.1557/JMR.1992.1564)
- [8] Šepitka J, Lukeš J, Staněk L, Filová E, Burdík Z, Rezníček J. Nanoindentation of intervertebral disc tissues localised by SHG imaging. *Comput Methods Biomech Biomed Eng.* 2012;15 Suppl 1:335–6. DOI: [10.1080/10255842.2012.713601](https://doi.org/10.1080/10255842.2012.713601)

Josef Šepitka, Ph.D.
Dept. of Mechanics, Biomechanics and Mechatronics
Faculty of Mechanical Engineering
Czech Technical University in Prague
Technická 4, CZ-160 00 Prague

E-mail: josef.sepitka@fs.cvut.cz
Phone: +420 224 352 649